Gauge Mediation Scenario with Hidden Sector Renormalization in MSSM

M. Arai– Czech Technical University in Prague
S. Kawai – Institute for the Early Universe (IEU)
N. Okada – University of Alabama

Citation of published version:

Arai, M., Kawai, S., Okada, N. (2010): Gauge Mediation Scenario with Hidden Sector Renormalization in MSSM. *Physical Review D,* 81(3).
DOI: https://doi.org/10.1103/PhysRevD.81.035022

PHYSICAL REVIEW D **81,** 035022 (2010)

Gauge mediation scenario with hidden sector renormalization in MSSM

Masato Arai,[1,*] Shinsuke Kawai,[2,3,†] and Nobuchika Okada[4,‡]

[1]*Institute of Experimental and Applied Physics, Czech Technical University in Prague, Horská 3a/22, 128 00 Prague 2, Czech Republic*

[2]*Institute for the Early Universe (IEU), 11-1 Daehyun-dong, Seodaemun-gu, Seoul 120-750, Korea*

[3]*Department of Physics, Sungkyunkwan University, Suwon 440-746, Korea*

[4]*Department of Physics and Astronomy, University of Alabama, Tuscaloosa, Alabama 35487, USA*

(Received 15 January 2010; published 26 February 2010)

We study the hidden sector effects on the mass renormalization of a simplest gauge-mediated supersymmetry breaking scenario. We point out that possible hidden sector contributions render the soft scalar masses smaller, resulting in drastically different sparticle mass spectrum at low energy. In particular, in the $\mathbf{5} + \bar{\mathbf{5}}$ minimal gauge-mediated supersymmetry breaking with high messenger scale (that is favored by the gravitino cold dark matter scenario), we show that a stau can be the next lightest superparticle for moderate values of hidden sector self-coupling. This provides a very simple theoretical model of long-lived charged next lightest superparticles, which imply distinctive signals in ongoing and upcoming collider experiments.

DOI: 10.1103/PhysRevD.81.035022 PACS numbers: 12.60.Jv, 11.10.Hi, 14.80.Ly, 98.80.Ft

I. INTRODUCTION

The minimal supersymmetric standard model (MSSM) is an attractive framework of a theory beyond the standard model. It resolves some of the shortcomings of the standard model and at the same time makes falsifiable predictions for upcoming experiments. The presence of dark matter, for instance, has been consolidated by numerous cosmological and astrophysical observations [1]. According to the best-fit Λ-cold dark matter (the ''concordance'') model, the major part of the energy density of the present universe is dark energy and dark matter, neither of them is explained by the standard model. While dark energy is likely to be of gravitational origin, dark matter is readily accommodated in MSSM; as the lightest superparticle (LSP) is protected by R parity, it is an ideal candidate of dark matter.

Among competing supersymmetry breaking scenarios of MSSM, the gauge-mediated supersymmetry breaking (GMSB) [2] is advantageous for natural suppression of flavor-changing neutral currents and CP violation. In GMSB the LSP is a gravitino. Cosmological model building with successful structure formation favors cold dark matter, which, in the case of gravitino dark matter, yields gravitino mass lower bound $m_{3/2} \gtrsim 100$ keV. The gravitino LSP of this mass range is realized by GMSB models with sufficiently high messenger scale (see also Sec. III). For this reason we will be concerned with the high messenger scale GMSB scenario in this paper. The interaction of the gravitino with the standard model particles is Planck-suppressed. While this makes the gravitino an ideal candidate of dark matter, it also makes its direct detection rather difficult. A more direct telltale of supersymmetry is from the next lightest superparticle (NLSP), which, in the case of GMSB, is either the lightest neutralino or the lightest charged slepton(s). In the high messenger scale GMSB, the NLSP is long-lived, behaving as quasistable particles, and the distinction of whether the NLSP is a neutralino or slepton leads to entirely different physics. In the ''minimal'' GMSB scenario based on the $N_5 = 1$ (the sum of the Dynkin indices) $\mathbf{5} + \bar{\mathbf{5}}$ messengers which are representations of the $SU(5)$ gauge group [3,4], the NLSP is a neutralino. The long-lived neutralino NLSP scenario is strongly constrained by the big-bang nucleosynthesis (BBN) [5], leading to severe constraints on both gravitino and neutralino masses. Assuming nonthermal production of gravitino dark matter combined with the BBN bound, the neutralino mass is constrained to be larger than the TeV scale. In contrast, if the gravitino dark matter is of thermal origin the neutralino mass can be smaller. In any case, the long-lived neutralino behaves like stable particles in collider experiments and the physics is similar to that of the neutralino LSP. If the NLSP is charged slepton(s), on the other hand, we expect entirely different signals. A natural candidate for a charged NLSP is the lightest scalar tau (stau). While the stau NLSP scenario is also constrained by BBN [5], the restrictions on the gravitino and stau masses are not so tight as the neutralino NLSP case. In collider experiments, charged particles like the stau leave tracks in detectors, allowing direct observations of the NLSP. It would also be possible to make a precise measurement of its mass, and the absence of missing energy (such as due to neutinos) would facilitate detailed study of various processes involving the stau [6–10]. In GMSB, the stau NLSP is obtained in models with larger N_5 [3,4] or messengers belonging to larger gauge groups [11]. The messenger index N_5, however, cannot be taken to

*Masato.Arai@utef.cvut.cz
†kawai@skku.edu
‡okadan@ua.edu

be arbitrarily large as it is constrained by the condition that the successful gauge group unification must be preserved. In the case of simple multiple $SU(5)$ messengers, for example, the possible range of N_5 is roughly $N_5 \lesssim 10$ for the messenger masses $\approx 10^{10}$ GeV. For too large N_5 the gauge couplings diverge before the unification.

These studies are based on the traditional assumption that the renormalization group (RG) flow of the visible world masses does not depend on details of the hidden sector dynamics, which, as is realized recently [12,13], turned out not necessarily to be the case. Based on this observation, effects of the hidden sector on the renormalization group equations (RGEs) are studied in [14]. The authors use a toy model of the hidden sector with a self-interaction coupling in the constrained MSSM, and show that the soft mass spectrum at low energy is altered by hidden sector effects, suggesting that such spectra can be used to determine the hidden scale and the strength of the self-coupling. In the present paper we shall carry out a similar analysis on the GMSB scenario that gives rise to gravitino cold dark matter, by taking into account the contributions from the hidden sector and reexamining the RG analysis of the minimal GMSB [3,4]. We find that the effect of the renormalized self-interaction coupling of the hidden sector field renders the soft scalar masses smaller than the conventional GMSB results, and consequently the low energy mass spectrum of the MSSM particles can be drastically altered. A phenomenologically interesting consequence of our analysis is that the stau can be the NLSP even in the minimal GMSB scenario. Our model thus provides a simple stau NLSP model with gravitino cold dark matter.

The plan of the paper is as follows. In the next section we present the setup of our model, focusing on how the hidden sector dynamics contributes to the RG of the visible sector. In Sec. III we present our numerical results, and in Sec. IV we discuss constraints of the parameter space from the collider and cosmological experiments. We conclude in Sec. V with comments, and explicit forms of the hidden sector contributions to the RGEs are summarized in the Appendix.

II. THE HIDDEN SECTOR IN THE GAUGE-MEDIATED SUPERSYMMETRY BREAKING

In the GMSB scenario, the messengers couple directly to the hidden sector fields (which is responsible for the supersymmetry breaking), and indirectly to the MSSM matter fields through the standard model gauge interactions. Once the supersymmetry is broken in the hidden sector, the gauginos and the scalars in the MSSM become massive via one-loop and two-loop corrections, respectively. In the minimal GMSB based on the $N_5 = 1$ $\mathbf{5} + \bar{\mathbf{5}}$ messenger belonging to an $SU(5)$, the gaugino masses at the messenger scale M are given by

$$M_a(t=0) = \frac{\alpha_a(M)}{4\pi}\Lambda, \tag{1}$$

where

$$\alpha_a = \frac{g_a^2}{4\pi}, \tag{2}$$

$t = \ln(\mu/M)$, and $\Lambda = F/M$ with F the supersymmetry breaking scale. The index $a = 1, 2, 3$ is for the MSSM gauge groups $U(1)$, $SU(2)$, $SU(3)$, and g_a are the corresponding gauge couplings. The soft scalar masses at the messenger scale are given by

$$m_i^2(t=0) = 2\Lambda^2 \sum_{a=1}^{3} C_2^a(R_i)\left(\frac{\alpha_a(M)}{4\pi}\right)^2, \tag{3}$$

where the index i denotes the MSSM scalars $(\tilde{q}, \tilde{u}, \tilde{d}, \tilde{l}, \tilde{e}, H_u, H_d)$ in this order, and $C_2^a(R_i)$ are the quadratic Casimir for the matter fields in representation R_i of the ath MSSM gauge group. As indicated, these masses are generated at the messenger scale M. Physical masses at the electroweak scale are evaluated through RG evolution. Below we follow [13,14] and derive the RGEs, taking the hidden sector effects into account.

We model the hidden sector by a single chiral superfield X with Lagrangian,

$$\mathcal{L}_{\text{hid}} = \int d^4\theta X^\dagger X + \left(\int d^2\theta \mathcal{W} + \text{H.c.}\right), \tag{4}$$

where the superpotential is

$$\mathcal{W} = \frac{\lambda}{3}X^3. \tag{5}$$

This does not itself break the supersymmetry but we assume that the F-term component of X acquires a nonzero vacuum expectation value by some mechanism. We shall be interested in the effects of the hidden sector renormalization. The hidden sector field X couples only to the messenger fields, and the messenger fields couple to the MSSM fields through the gauge interactions. Below the messenger scale M, the messenger fields are integrated out, yielding the following effective interactions between X and the MSSM fields,

$$\mathcal{L}_{\text{int}} = k_i \int d^4\theta \frac{XX^\dagger}{M^2}\Phi_i\Phi_i^\dagger + \left(w_a \int d^2\theta \frac{X}{M} W^{a\alpha}W_\alpha^a + \text{H.c.}\right), \tag{6}$$

with real and complex coefficients k_i and w_a. Here Φ_i are the MSSM matter superfields (their scalar components are $\phi_i = \tilde{q}, \tilde{u}, \tilde{d}, \tilde{l}, \tilde{e}, H_u, H_d$), and W_α^a are the MSSM field strengths. As the F-term component of X obtains a nonzero vacuum expectation value at the messenger scale M, the first and the second terms of (6), respectively, give the scalar masses (3) and the gaugino masses (1).

Let us consider quantum corrections to (6). There are no 1 particle irreducible diagrams that renormalize operators linear in X, and hence the second line of (6) receives only the wave function renormalization coming from the hidden sector field. By the renormalization $X \to Z_X^{-1/2} X$, the second line of (6) becomes

$$w_a \int d^2\theta Z_X^{-1/2} \frac{X}{M} W^{a\alpha} W^a_\alpha + \text{H.c.} \tag{7}$$

The integrand is a holomorphic function, whereas the factor $Z_X^{-1/2}$ is real. Therefore, due to the nonrenormalization theorem [15,16], there is no quantum correction in the second line in (6). This means that w_a does not receive any quantum correction at all scales. On the other hand, the integrand of the first term in (6) is not a holomorphic function, and therefore the coefficients k_i are renormalized by the visible sector gauge interactions and the hidden sector coupling λ in (5). They then satisfy the RGEs

$$\frac{d}{dt} k_i(t) = \gamma(t) k_i(t) - \frac{1}{16\pi^2} \sum_{a=1}^{3} 8 C_2^a(R_i) g_a^6(t) G_a,$$
$$G_a \equiv w_a w_a^\dagger. \tag{8}$$

The second term is the leading visible sector contribution. In the first term $\gamma(t)$ is the anomalous dimension at $t = \ln(\mu/M)$ arising from the hidden sector interactions (5). The anomalous dimension in the lowest order in λ is

$$\gamma(t) = \frac{\lambda(t)\lambda^\dagger(t)}{2\pi^2}, \tag{9}$$

where $\lambda(t)$ is the running hidden sector Yukawa coupling which renormalizes according to

$$\frac{d\lambda(t)}{dt} = \frac{3}{8\pi^2} \lambda^3(t). \tag{10}$$

The RGEs (8) are solved as

$$k_i(t) = \exp\left(- \int_t^0 dt' \gamma(t') \right) k_i(0) + \frac{1}{16\pi^2} \sum_{a=1}^{3} 8 C_2^a(R_i)$$
$$\times \int_t^0 ds g_a^6(s) \exp\left(- \int_t^s dt' \gamma(t') \right) G_a. \tag{11}$$

Using this expression, the scalar masses of the visible sector including the RG effects are described by

$$m_i^2(t) = k_i(t) \Lambda^2, \tag{12}$$

with

$$k_i(0) = 2 \sum_{a=1}^{3} \left(\frac{\alpha_a(M)}{4\pi} \right)^2 C_2^a(R_i). \tag{13}$$

Here the gauge couplings run according to the standard 1-loop formula,

$$\frac{1}{\alpha_a(\mu)} = \begin{cases} \frac{1}{\alpha_a(M_Z)} - \frac{1}{2\pi} b_a \ln \frac{M_S}{M_Z} - \frac{1}{2\pi} b_a^S \ln \frac{\mu}{M_S}, & (\mu > M_S) \\ \frac{1}{\alpha_a(M_Z)} - \frac{1}{2\pi} b_a \ln \frac{\mu}{M_Z}, & (\mu \le M_S), \end{cases} \tag{14}$$

where $(b_1^S, b_2^S, b_3^S) = (-3, 1, 33/5)$ for the MSSM and $(b_1, b_2, b_3) = (-7, -19/6, 41/10)$ for the standard model gauge couplings. M_Z and M_S are the Z-boson mass and a typical soft mass scale, respectively.

III. THE HIDDEN SECTOR RENORMALIZATION GROUP FLOW

We shall be interested in the low energy mass spectra, in particular, determination of the NLSP. The hidden sector renormalization affects the mass RG flows between the messenger scale $\mu = M$ and the hidden scale $\mu = M_{\text{hid}}$. Equation (8) implies that the RGEs for the MSSM soft scalar masses are modified as

$$\frac{dm_i^2}{dt} \to \frac{dm_i^2}{dt} + \frac{\lambda\lambda^\dagger}{2\pi^2} m_i^2, \tag{15}$$

while those for the other masses and couplings are unaltered (see, for example, [17]). Below the hidden scale, the hidden sector fields are integrated out and all the masses and the couplings evolve according to the standard MSSM RGEs. The low energy mass spectrum is obtained by integrating the RGEs, from the messenger scale to the hidden scale with the hidden sector effects (15) included, and then down to the electroweak scale in the standard way. In this section we present numerical study of the MSSM RGEs including the hidden sector effects at one-loop order. The nonstandard parts of the RGEs are listed in the Appendix.

In our computations we made following approximations. For simplicity only the (3, 3) family component of the three Yukawa matrices, and only the (3, 3) family component of the trilinear A-term matrices, are set to be nonzero. The latter are set to vanish at the messenger scale. Throughout our analysis we use following values: $\tan\beta = 10$, the soft mass scale $M_S = 500$ GeV, and $\Lambda = F/M = 10^5$ GeV. The hidden sector scale is defined as $M_{\text{hid}} = \sqrt{F} = \sqrt{\Lambda \times M}$. For instance, for $M = 10^{12}$ GeV, the hidden scale is $M_{\text{hid}} = 10^{8.5}$ GeV.

Figure 1 shows the mass RG flows of the first and the third generation sleptons with and without the hidden sector effects, and Fig. 2 shows similar results for the squarks. The messenger scale is taken to be $M = 10^{12}$ GeV. In both Figs. 1 and 2, we see that the hidden sector renormalization (down to the hidden scale M_{hid}) gives rise to smaller soft scalar masses, compared to the flows without it. This effect is readily understood by looking at the RGEs (A1)–(A7), in which the effects of the

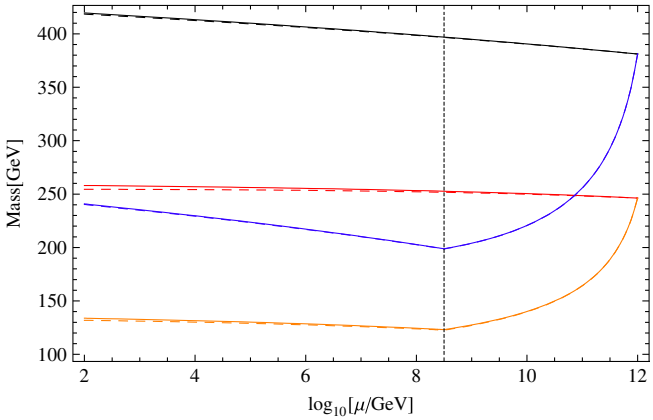

FIG. 1 (color online). The slepton mass RG flows with and without the hidden sector effects. The (black and blue) curves originating from 381 GeV [the mass set by Eq. (3)] at the messenger scale 10^{12} GeV are the left-handed, and the curves from 246 GeV (red and orange) are the right-handed sleptons. The solid and dashed curves indicate the first and third generation sleptons. The curves with the sharp decline (blue and orange) down to the hidden scale $M_{\rm hid} = 10^{8.5}$ GeV (the vertical dotted line) are the flows including the hidden sector effects. The nearly straight curves (black and red) are the flows without the hidden sector effects. We have chosen $M = 10^{12}$ GeV, $\lambda = 3.8$, and $\tan\beta = 10$.

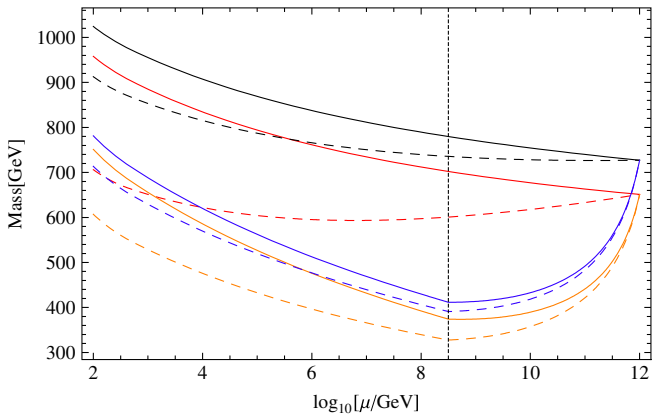

FIG. 2 (color online). The squark mass RG flows with and without the hidden sector effects. The (black and blue) curves starting from 727 GeV [the mass set by Eq. (3)] at the messenger scale $M = 10^{12}$ GeV are the left-handed squarks, and those starting from the smaller mass 651 GeV (red and orange) are the right-handed up-type squarks. The first and the third generations are, respectively, denoted by the solid and the dashed curves. The (blue and orange) curves with the sharp decline from the messenger scale down to the hidden scale $M_{\rm hid} = 10^{8.5}$ GeV (the dotted vertical line) are the flows with the hidden sector effects, whereas the (black and red) curves emanating to the left from the messenger scale are the flows without the hidden sector effects. The parameters are the same as in Fig. 1 ($\lambda = 3.8$ and $\tan\beta = 10$).

hidden sector renormalization are the positive terms $4\lambda^2 m_i^2$ on the right-hand sides.[1] It is also obvious from the RGEs that larger λ gives smaller soft scalar masses at low energy. In contrast, the RGEs and hence the low energy mass spectrum of the gauginos are not affected by the hidden sector renormalization. This implies that the lightest scalar superparticle, namely, the lightest stau, can be lighter than the lightest gaugino, i.e., bino, for sufficiently large λ. In Fig. 3, we plot the stau/neutralino mass ratio $m_{\tilde\tau}/m_{\tilde\chi^0}$ at the electroweak scale as a function of λ with $M = 10^{12}$ GeV. $\lambda = 0$ corresponds to no hidden sector RG effects, reproducing the known result of the neutralino NLSP in the minimal GMSB scenario. As λ is increased,[2] the mass $m_{\tilde\tau}$ of the lightest stau $\tilde\tau$ becomes smaller, while the neutralino mass $m_{\tilde\chi^0}$ remains the same; the stau becomes lighter than the neutralino when $\lambda \gtrsim 3.7$. For example, $M = 10^{12}$ GeV and $\lambda = 3.8$ yield $m_{\tilde\tau} = 132$ GeV and the neutralino (bino) mass $m_{\tilde\chi^0} = 135$ GeV at the electroweak scale. This stau mass is compatible with the LEP bound for long-lived massive charged particles $\gtrsim 102.0$ GeV [18].

The ratio of the stau and the bino masses $m_{\tilde\tau}/m_{\tilde\chi^0}$ is depicted in Fig. 4, against the messenger scale M for various values of λ. The vertical dashed line indicates the minimal messenger scale determined by the condition that the gravitino is cold dark matter, $m_{3/2} \gtrsim 0.1$ MeV. Here the gravitino mass is given by [19,20]

$$m_{3/2} \sim \frac{F}{\sqrt{3}M_P} = \frac{M}{\sqrt{3}M_P}\Lambda, \tag{16}$$

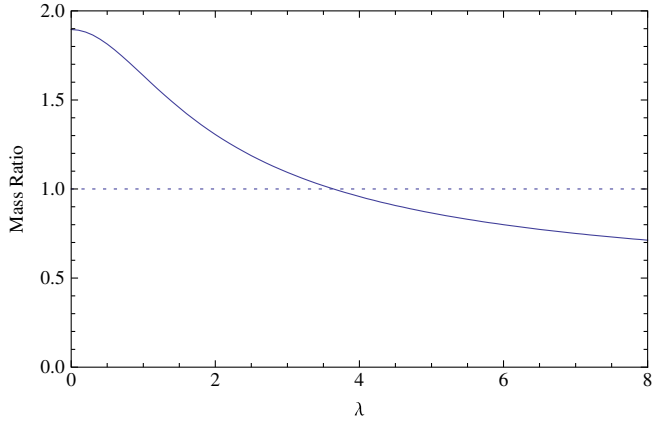

FIG. 3 (color online). The stau/neutralino mass ratio $m_{\tilde\tau}/m_{\tilde\chi^0}$ plotted against the hidden sector coupling λ. We used $M = 10^{12}$ GeV and $\tan\beta = 10$.

[1]In GMSB a hidden sector field needs to be a MSSM gauge singlet, and a possible model of hidden sector superpotential is a Yukawa type, as in (5). Then the hidden sector contributions to RGEs are always positive.

[2]The perturbative means are valid for $\lambda^2/(4\pi) \lesssim 1$. Our choice of the parameter in the following discussions is roughly within this range.

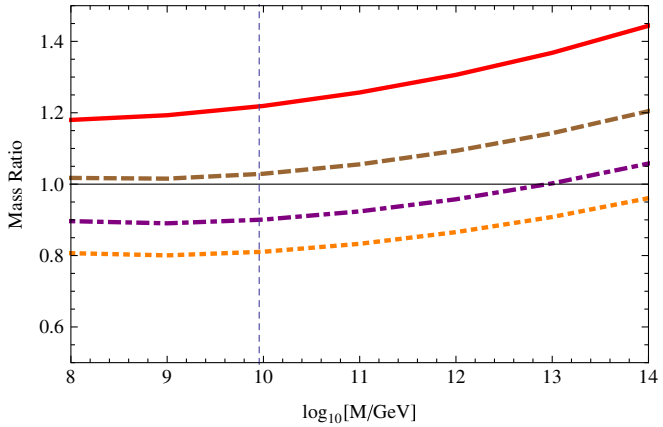

FIG. 4 (color online). The stau/neutralino mass ratio $m_{\tilde{\tau}}/m_{\tilde{\chi}^0}$ plotted against the messenger scale M, for $\lambda = 2$ (solid red line), $\lambda = 3$ (dashed brown), $\lambda = 4$ (dash-dotted purple), $\lambda = 5$ (dotted orange) from above, with $\tan\beta = 10$. The vertical dashed line indicates the minimal messenger scale in our model, $M_* = 9.0 \times 10^9$ GeV. For large enough λ the stau becomes lighter than the neutralino.

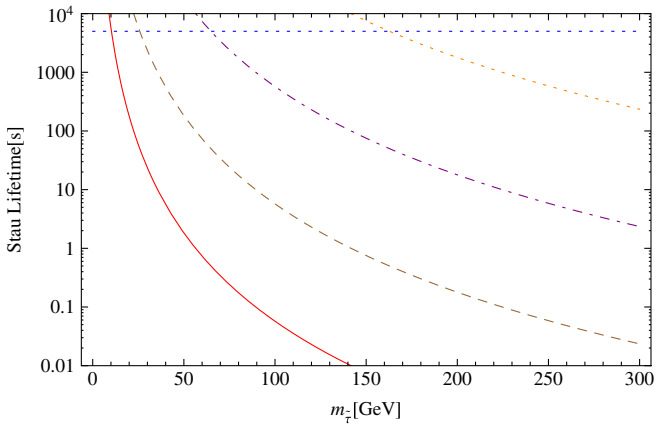

FIG. 5 (color online). Lifetime of the stau plotted against the stau mass, for $m_{3/2} = 1$ MeV (red solid curve), $m_{3/2} = 10$ MeV (brown dashed), $m_{3/2} = 0.1$ GeV (purple dash-dotted), and $m_{3/2} = 1$ GeV (orange dotted).

where $M_P = 2.4 \times 10^{18}$ GeV is the reduced Planck mass. The gravitino mass is also affected by the hidden sector renormalization [14]. For example, when the source of the supersymmetry breaking is a term linear in X, the vacuum expectation value of the F-term component of X is proportional to the wave function renormalization factor $Z_X^{-1/2} = \exp(-\frac{1}{2}\int_t^0 dt\gamma(t))$. This takes effect from the messenger scale down to the hidden scale, resulting in suppression of the gravitino mass by the factor $Z_X^{-1/2} \approx 0.5$ for $\lambda = 2 \sim 4$. Taking this suppression into account, the minimal messenger scale consistent with the cold dark matter condition $m_{3/2} \gtrsim 0.1$ MeV is $M_* \approx 9.0 \times 10^9$ GeV. By choosing an appropriate messenger scale M within $M_* \lesssim M \lesssim 10^{12}$ GeV, the stau can be the NLSP with λ as small as 3.0.

IV. STAU NLSP PHENOMENOLOGY

In the previous section we have seen that the hidden sector renormalization can change the low energy mass spectrum. Here we describe phenomenological implications when the NLSP is the lightest stau.

We note that cosmological constraints on the mass parameters in the stau NLSP scenario are less stringent than in the neutralino NLSP case [5]. In BBN, the stau produces a bound state with ^{4}He that tends to overproduce primordial ^{6}Li through catalytic reaction $^4\mathrm{He}\tilde{\tau}^- + \mathrm{D} \to {}^6\mathrm{Li} + \tilde{\tau}^-$ [21,22] (see also [5,23,24]), giving upper bound for the stau lifetime[3]

$$\tau_{\tilde{\tau}} = \Gamma^{-1}(\tilde{\tau} \to \tau\tilde{G}) \simeq \frac{48\pi m_{3/2}^2 M_P^2}{m_{\tilde{\tau}}^5}\left(1 - \frac{m_{3/2}^2}{m_{\tilde{\tau}}^2}\right)^{-4} \simeq 5.7 \times 10^4 \left(\frac{m_{3/2}}{1\ \mathrm{GeV}}\right)^2 \left(\frac{100\ \mathrm{GeV}}{m_{\tilde{\tau}}}\right)^5 \lesssim 5 \times 10^3\ \text{seconds}. \quad (17)$$

Figure 5 shows the stau lifetime $\tau_{\tilde{\tau}}$ plotted against the stau mass $m_{\tilde{\tau}}$ for different values of gravitino mass $m_{3/2}$. The upper bound of the stau lifetime $\tau_{\tilde{\tau}} \lesssim 5 \times 10^3$ constrains the gravitino mass from above. For our typical range of the stau mass $m_{\tilde{\tau}} \approx 130$ GeV, the gravitino mass is $m_{3/2} \lesssim 0.6$ GeV. Together with the condition that the gravitino behaves as cold dark matter, a successful cosmological scenario with the stau NLSP and gravitino cold dark matter requires the gravitino mass to be within 0.1 MeV $\lesssim m_{3/2} \lesssim 0.6$ GeV. The model prediction (16) is safely within this range.

The origin of the relic gravitino is either thermal or nonthermal production. The thermal production is due to scattering in the thermal plasma in the radiation dominated era after inflation. The relic abundance from this contribution is computed as [26–28]

$$\Omega_{\tilde{G}}^{\mathrm{TP}} h^2 \simeq 0.3 \left(\frac{T_R}{10^{10}\ \mathrm{GeV}}\right)\left(\frac{100\ \mathrm{GeV}}{m_{3/2}}\right)\left(\frac{M_3}{1\ \mathrm{TeV}}\right)^2, \quad (18)$$

where T_R is the reheating temperature and h is the Hubble constant in the unit of 100 km Mpc^{-1} s^{-1}. The nonthermal production of the gravitino is due to decay of the NLSP [38,39].[4] The abundance of nonthermally produced grav-

[3]This constraint may be relaxed by considering substantial left-right mixing of the stau mass eigenstates [25].

[4]The productions of gravitinos from decay of moduli, inflation, and Polonyi fields have also been discussed [29–37].

itinos is estimated as [40–43]

$$\Omega_{\tilde{G}}^{\mathrm{NTP}}h^2 = \frac{m_{3/2}}{m_{\tilde{\tau}}}\Omega_{\tilde{\tau}}^{\mathrm{th}}h^2 \simeq 0.02\left(\frac{m_{3/2}}{100\ \mathrm{GeV}}\right)\left(\frac{m_{\tilde{\tau}}}{1\ \mathrm{TeV}}\right), \quad (19)$$

where $\Omega_{\tilde{\tau}}^{\mathrm{th}}$ is the thermal abundance of the stau. The total gravitino abundance is thus

$$\Omega_{\tilde{G}}h^2 = \Omega_{\tilde{G}}^{\mathrm{TP}}h^2 + \Omega_{\tilde{G}}^{\mathrm{NTP}}h^2, \quad (20)$$

which is constrained by the observed dark matter density [1]

$$\Omega_{\tilde{G}}h^2 \leq \Omega_{\mathrm{CDM}}h^2 \simeq 0.1131 \pm 0.0034. \quad (21)$$

For stau mass $m_{\tilde{\tau}} \approx 130$ GeV, the BBN bound for the gravitino mass $m_{3/2} \lesssim 0.6$ GeV restricts the nonthermally produced gravitino abundance (19) to be extremely small, $\Omega_{\tilde{G}}^{\mathrm{NTP}}h^2 \lesssim 10^{-5}$, indicating that most of the gravitino dark matter is produced thermally. The BBN bound for the gravitino mass and the dark matter abundance (21) gives an upper bound of the reheating temperature. Using (18), we find $T_R \lesssim 10^7$ GeV. The model prediction (16) with $M = 10^{12}$ GeV and $\Lambda = 10^5$ GeV yields $m_{3/2} \approx 11$ MeV; if the right amount of gravitino dark matter of this mass is to be produced thermally ($\Omega_{\mathrm{CDM}} = \Omega_{\tilde{G}}^{\mathrm{TP}}$), one needs $T_R \approx 10^6$ GeV. This is lower than the reheating temperature required for successful leptogenesis; the observed baryon asymmetry needs to be generated by some other mechanism, such as [44].

Stau NLSP is also of interest for collider phenomenology. Equation (17) implies that the lifetime of the stau $\tau_{\tilde{\tau}}$ may be long, depending on the gravitino and stau masses; for instance, $\tau_{\tilde{\tau}} \approx 100$ sec for $m_{\tilde{\tau}} = 130$ GeV and $m_{3/2} = 0.1$ GeV. For a particle with such a long lifetime, the decay length well exceeds the size of detectors and the decay takes place outside detectors. There have been intriguing proposals for trapping such long-lived charged NLSPs outside detectors [6–10]. It has been pointed out that detailed studies of stau decay may provide precise measurements of the gravitino mass and the supersymmetry breaking scale. This would also be a crucial test of supergravity since the stau decay $\tilde{\tau} \to \tau\tilde{G}$ involves supergravity effects.

V. DISCUSSION

In this paper we studied the effects of hidden sector renormalization in the minimal GMSB model, using a toy model of the hidden sector field X with self-coupling λ. We saw that the soft scalar and gravitino masses are affected by the hidden sector RG; they become smaller than the conventional GMSB RG results. Since the gaugino masses are unaltered, the resulting low energy mass spectrum of the superparticles can be quite different from the conventional GMSB. In particular, we find that the stau, instead of the neutralino, can be the NLSP in the minimal GMSB model. Based on this observation we also discussed phenomenological implications of the stau NLSP and gravitino cold dark matter arising from the model. With our typical choice of parameter values, the messenger scale $M = 10^{12}$ GeV, $\tan\beta = 10$, $\Lambda = F/M = 10^5$ GeV and the hidden sector coupling $\lambda = 3.8$, the model yields stau NLSP with mass $m_{\tilde{\tau}} \approx 130$ GeV. The gravitino mass arising from these parameter values is shown to be consistent with the BBN constraints. It was also shown that gravitino cold dark matter with observationally consistent abundance is attributed to thermal production in this scenario.

We comment that the hidden sector dependence of the mass spectra, as discussed in this paper, does not necessarily mar the predictability of the GMSB scenario. Rather, the hidden sector only influences the soft scalar and the gravitino masses, and the beauty of the GMSB scenario is kept intact. In fact, as emphasized in [12–14], the effects of the hidden sector RG can be viewed as a new window to look into the hidden sector using the low energy mass spectrum that is expected to be revealed in experiments such as the Large Hadron Collider. While the model discussed here represents a simple toy example of many possible hidden sector models, we believe essential features of our results to be generic. For example, only the soft scalar and the gravitino masses, and not the other masses or the couplings, are subject to the hidden sector RG effects. This is a consequence of the powerful nonrenormalization theorem, and we do not expect this feature to be dependent on details of the hidden sector. Needless to say, however, there might be various other model-dependent issues that deserve further study.

ACKNOWLEDGMENTS

This work was supported in part by the Research Program MSM6840770029 and by the project of International Cooperation ATLAS-CERN of the Ministry of Education, Youth, and Sports of the Czech Republic (M. A.), and the WCU Grant No. R32-2008-000-10130-0 (S. K.).

APPENDIX: THE RENORMALIZATION GROUP EQUATIONS

In this Appendix we list the RGEs for the soft mass parameters that involve the hidden sector contributions. The new ingredient is the hidden-visible interaction (5), which gives additional terms to the soft mass RGEs. Within our approximation only the (3, 3) family component of the three Yukawa matrices, y_t, y_b, y_τ, are set to be nonzero. The corresponding nonzero components of the three trilinear A-term matrices are a_t, a_b, a_τ. We use normalized variables $A_t = a_t/y_t$, $A_b = a_b/y_b$, $A_\tau = a_\tau/y_\tau$.

The RGEs for the soft masses are

$$8\pi^2 \frac{dm_Q^2}{dt} = \xi_t + \xi_b - \frac{16}{3} g_3^2 M_3^2 - 3 g_2^2 M_2^2 - \frac{1}{15} g_1^2 M_1^2 + \frac{1}{5} g_1^2 \xi_1 + 4\lambda^2 m_Q^2, \quad \text{(A1)}$$

$$8\pi^2 \frac{dm_U^2}{dt} = 2\xi_t - \frac{16}{3} g_3^2 M_3^2 - \frac{16}{15} g_1^2 M_1^2 - \frac{4}{5} g_1^2 \xi_1 + 4\lambda^2 m_U^2, \quad \text{(A2)}$$

$$8\pi^2 \frac{dm_D^2}{dt} = 2\xi_b - \frac{16}{3} g_3^2 M_3^2 - \frac{4}{15} g_1^2 M_1^2 + \frac{2}{5} g_1^2 \xi_1 + 4\lambda^2 m_D^2, \quad \text{(A3)}$$

$$8\pi^2 \frac{dm_L^2}{dt} = \xi_\tau - 3 g_2^2 M_2^2 - \frac{3}{5} g_1^2 M_1^2 - \frac{3}{5} g_1^2 \xi_1 + 4\lambda^2 m_L^2, \quad \text{(A4)}$$

$$8\pi^2 \frac{dm_E^2}{dt} = 2\xi_\tau - \frac{12}{5} g_1^2 M_1^2 + \frac{6}{5} g_1^2 \xi_1 + 4\lambda^2 m_E^2, \quad \text{(A5)}$$

$$8\pi^2 \frac{dm_{H_u}^2}{dt} = 3\xi_t - 3 g_2^2 M_2^2 - \frac{3}{5} g_1^2 M_1^2 + \frac{3}{5} g_1^2 \xi_1 + 4\lambda^2 m_{H_u}^2, \quad \text{(A6)}$$

$$8\pi^2 \frac{dm_{H_d}^2}{dt} = 3\xi_b + \xi_\tau - 3 g_2^2 M_2^2 - \frac{3}{5} g_1^2 M_1^2 - \frac{3}{5} g_1^2 \xi_1 + 4\lambda^2 m_{H_d}^2, \quad \text{(A7)}$$

where

$$\xi_t = y_t^2 (m_{H_u}^2 + m_Q^2 + m_U^2 + A_t^2), \quad \text{(A8)}$$

$$\xi_b = y_b^2 (m_{H_d}^2 + m_Q^2 + m_D^2 + A_b^2), \quad \text{(A9)}$$

$$\xi_\tau = y_\tau^2 (m_{H_d}^2 + m_L^2 + m_E^2 + A_\tau^2), \quad \text{(A10)}$$

and

$$\xi_1 = \tfrac{1}{2}\{m_{H_u}^2 - m_{H_d}^2 + \mathrm{Tr}(m_Q^2 - 2m_U^2 + m_D^2 + m_E^2 - m_L^2)\}. \quad \text{(A11)}$$

Here the trace means the sum over the generations. The above equations for the squarks and sleptons apply to the third family; the equations for the first and the second families are obtained from above by simply omitting the Yukawa and the A-term contributions (i.e., neglecting the ξ_t, ξ_b, ξ_τ terms). All the other RGEs (the gauge couplings, the gaugino masses, the Yukawa couplings, and the A terms) are unaffected and are given, e.g., in [17].

[1] E. Komatsu *et al.* (WMAP), Astrophys. J. Suppl. Ser. **180**, 330 (2009).
[2] M. Dine, W. Fischler, and M. Srednicki, Nucl. Phys. **B189**, 575 (1981); S. Dimopoulos and S. Raby, Nucl. Phys. **B192**, 353 (1981); L. Alvarez-Gaume, M. Claudson, and M. B. Wise, Nucl. Phys. **B207**, 96 (1982); M. Dine and W. Fischler, Nucl. Phys. **B204**, 346 (1982); C. R. Nappi and B. A. Ovrut, Phys. Lett. **113B**, 175 (1982); M. Dine and A. E. Nelson, Phys. Rev. D **48**, 1277 (1993); M. Dine, A. E. Nelson, and Y. Shirman, Phys. Rev. D **51**, 1362 (1995); M. Dine, A. E. Nelson, Y. Nir, and Y. Shirman, Phys. Rev. D **53**, 2658 (1996).
[3] S. Dimopoulos, M. Dine, S. Raby, and S. D. Thomas, Phys. Rev. Lett. **76**, 3494 (1996).
[4] S. Dimopoulos, S. D. Thomas, and J. D. Wells, Nucl. Phys. **B488**, 39 (1997).
[5] M. Kawasaki, K. Kohri, T. Moroi, and A. Yotsuyanagi, Phys. Rev. D **78**, 065011 (2008).
[6] W. Buchmuller, K. Hamaguchi, M. Ratz, and T. Yanagida, Phys. Lett. B **588**, 90 (2004).
[7] J. L. Feng, A. Rajaraman, and F. Takayama, Int. J. Mod. Phys. D **13**, 2355 (2004).
[8] K. Hamaguchi, Y. Kuno, T. Nakaya, and M. M. Nojiri, Phys. Rev. D **70**, 115007 (2004).
[9] J. L. Feng and B. T. Smith, Phys. Rev. D **71**, 015004 (2005).
[10] K. Hamaguchi, M. M. Nojiri, and A. de Roeck, J. High Energy Phys. 03 (2007) 046.
[11] R. N. Mohapatra, N. Okada, and H.-B. Yu, Phys. Rev. D **78**, 075011 (2008).
[12] M. Dine *et al.*, Phys. Rev. D **70**, 045023 (2004).
[13] A. G. Cohen, T. S. Roy, and M. Schmaltz, J. High Energy Phys. 02 (2007) 027.
[14] B. A. Campbell, J. Ellis, and D. W. Maybury, arXiv:0810.4877.
[15] N. Seiberg, Phys. Lett. B **318**, 469 (1993).
[16] K. A. Intriligator, R. G. Leigh, and N. Seiberg, Phys. Rev. D **50**, 1092 (1994).
[17] D. J. Castano, E. J. Piard, and P. Ramond, Phys. Rev. D **49**, 4882 (1994).
[18] G. Abbiendi *et al.* (OPAL), Phys. Lett. B **572**, 8 (2003).
[19] S. Deser and B. Zumino, Phys. Rev. Lett. **38**, 1433 (1977).
[20] E. Cremmer *et al.*, Phys. Lett. **79B**, 231 (1978).
[21] M. Pospelov, Phys. Rev. Lett. **98**, 231301 (2007).
[22] R. H. Cyburt, J. R. Ellis, B. D. Fields, K. A. Olive, and V. C. Spanos, J. Cosmol. Astropart. Phys. 11 (2006) 014.
[23] K. Kohri and F. Takayama, Phys. Rev. D **76**, 063507 (2007).

[24] M. Kaplinghat and A. Rajaraman, Phys. Rev. D **74**, 103004 (2006).
[25] M. Ratz, K. Schmidt-Hoberg, and M. W. Winkler, J. Cosmol. Astropart. Phys. 10 (2008) 026.
[26] M. Bolz, A. Brandenburg, and W. Buchmuller, Nucl. Phys. **B606**, 518 (2001).
[27] J. Pradler and F. D. Steffen, Phys. Rev. D **75**, 023509 (2007).
[28] F. D. Steffen, J. Cosmol. Astropart. Phys. 09 (2006) 001.
[29] M. Hashimoto, K. I. Izawa, M. Yamaguchi, and T. Yanagida, Prog. Theor. Phys. **100**, 395 (1998).
[30] R. Kallosh, L. Kofman, A. D. Linde, and A. Van Proeyen, Phys. Rev. D **61**, 103503 (2000).
[31] G. N. Felder, L. Kofman, and A. D. Linde, Phys. Rev. D **60**, 103505 (1999).
[32] A. L. Maroto and A. Mazumdar, Phys. Rev. Lett. **84**, 1655 (2000).
[33] G. F. Giudice, I. Tkachev, and A. Riotto, J. High Energy Phys. 08 (1999) 009.
[34] M. Dine, W. Fischler, and D. Nemeschansky, Phys. Lett. **136B**, 169 (1984).
[35] G. D. Coughlan, R. Holman, P. Ramond, and G. G. Ross, Phys. Lett. **140B**, 44 (1984).
[36] I. Joichi and M. Yamaguchi, Phys. Lett. B **342**, 111 (1995).
[37] J. J. Heckman, A. Tavanfar, and C. Vafa, arXiv:0812.3155.
[38] J. L. Feng, A. Rajaraman, and F. Takayama, Phys. Rev. Lett. **91**, 011302 (2003).
[39] J. L. Feng, A. Rajaraman, and F. Takayama, Phys. Rev. D **68**, 063504 (2003).
[40] S. Borgani, A. Masiero, and M. Yamaguchi, Phys. Lett. B **386**, 189 (1996).
[41] T. Asaka, K. Hamaguchi, and K. Suzuki, Phys. Lett. B **490**, 136 (2000).
[42] F. D. Steffen, AIP Conf. Proc. **903**, 595 (2007).
[43] F. D. Steffen, arXiv:0711.1240.
[44] I. Affleck and M. Dine, Nucl. Phys. B **249**, 361 (1985).